

# Signatures of a quantum Griffiths phase in a d-metal alloy close to its ferromagnetic quantum critical point

Almut Schroeder<sup>1</sup>, Sara Ubaid-Kassis<sup>1</sup> and Thomas Vojta<sup>2</sup>

<sup>1</sup> Department of Physics, Kent State University, Kent OH 44242, USA

<sup>2</sup> Department of Physics, Missouri University of Science and Technology, Rolla MO 65409, USA

E-mail: aschroe2@kent.edu

**Abstract.** We report magnetization ( $M$ ) measurements close to the ferromagnetic quantum phase transition of the d-metal alloy  $\text{Ni}_{1-x}\text{V}_x$  at a vanadium concentration of  $x_c \approx 11.4\%$ . In the diluted regime ( $x > x_c$ ), the temperature ( $T$ ) and magnetic field ( $H$ ) dependencies of the magnetization are characterized by nonuniversal power laws and display  $H/T$  scaling in a wide temperature and field range. The exponents vary strongly with  $x$  and follow the predictions of a quantum Griffiths phase. We also discuss the deviations and limits of the quantum Griffiths phase as well as the phase boundaries due to bulk and cluster physics.

## 1. Introduction

Magnetic quantum phase transitions (QPT) have been studied in transition metal alloys and in heavy-fermion compounds tuned, e.g., by pressure or chemical substitution. They still offer challenges to theory and experiment (see Ref. [1] for a recent review). Quantum critical behavior is signified by singularities in thermodynamic and transport properties. Usually, specific power laws with characteristic exponents have been predicted at the quantum critical point (QCP) for “clean” homogeneous systems, while “disordered” inhomogeneous systems, driven, e.g., by chemical substitution, may show different behavior [2]. In the case of metallic (itinerant) Heisenberg magnets, a strong-disorder renormalization group [3] predicts an exotic infinite-randomness QCP accompanied by quantum Griffiths singularities [4]. At such a QCP, thermodynamic observables are expected to be singular not just at criticality but in a finite region around the QCP called the quantum Griffiths phase (GP). This region features power laws (e.g., in the magnetic susceptibility,  $\chi \sim T^{\lambda-1}$ , and the magnetization,  $M \sim H^\lambda$ ) characterized by a nonuniversal Griffiths exponent  $\lambda$  which varies with distance to the QCP. Quantum Griffiths singularities have attracted a lot of attention. Many heavy fermion compounds display anomalous power-laws in specific heat  $C(T)$  and  $\chi(T)$  [5]; and quantum Griffiths behavior was suggested as an explanation [6]. Recently, a more systematic variation of the exponents could be found at the ferromagnetic QPT of  $\text{CePd}_{1-x}\text{Rh}_x$  [7].

To avoid additional complications due to the Kondo effect and to study a larger energy scale we recently investigated the simple fcc transition metal alloy  $\text{Ni}_{1-x}\text{V}_x$  [8] as an example of an itinerant ferromagnet (FM) in which the transition temperature ( $T_c = 630\text{K}$  for pure Ni) can be tuned to zero by chemical substitution. As explained by Friedel [9] the “disorder” is introduced

because the charge contrast of the replacing vanadium atoms creates large defects yielding an inhomogeneous magnetization density. In contrast, diluting Ni with isoelectronic Pd does not lead to a strongly disordered scenario:  $\text{Ni}_{1-x}\text{Pd}_x$  remains ferromagnetic up to  $x_c = 0.975$  where it rather shows the signatures of a clean quantum critical point [10]. We showed in Ref. [11] that magnetization and susceptibility above the critical vanadium concentration  $x_c \approx 11.4\%$  where  $T_c$  is suppressed to 0 indeed follow simple power laws with nonuniversal exponents that confirm the quantum Griffiths scenario over a wide temperature and magnetic field regime. At very low temperatures, deviations from the quantum Griffiths scenario hint at a cluster glass phase. Here, we provide additional details not shown in Ref. [11]. We demonstrate that  $H/T$ -scaling holds for a wide concentration regime and show the scaling plots. In addition, we reveal how the impact of disorder is manifest in the original  $M$  data close to  $x_c$ , and we show the details of the determination of the phase boundaries in order to better distinguish bulk behavior from individual cluster physics in this inhomogeneous system.

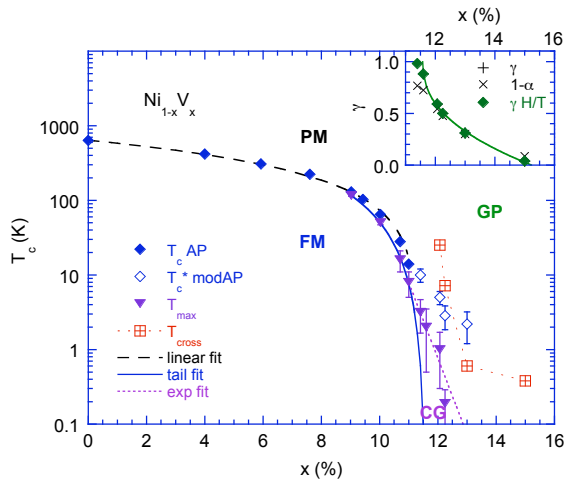


**Figure 1.** Temperature ( $T$ ) - concentration ( $x$ ) phase diagram of  $\text{Ni}_{1-x}\text{V}_x$  showing the ferromagnetic (FM), paramagnetic (PM), quantum Griffiths (GP) and cluster glass (CG) phases. Closed and open diamonds mark  $T_c$  and  $T_c^*$  as determined by linear and modified Arrott plots, respectively (data from [8] included). Triangles denote to  $T_{max}$  from maxima in susceptibility.  $T_{cross}$  is seen as lower limit of GP (see [11]). The dashed line is a linear extrapolation, the solid line is a tail fit describing the FM boundary, while the straight dotted line marks the onset of the CG. Inset shows the strong concentration  $x$ -variation of the exponent  $\gamma$  from  $\chi(T)$ ,  $\alpha - 1$  from  $M(H)$  and  $\gamma$  from the  $H/T$ -scaling plot in the GP.

## 2. Results

Magnetization and ac-susceptibility measurements were performed on polycrystalline  $\text{Ni}_{1-x}\text{V}_x$  samples with  $x = 9 - 15\%$  as described in Ref. [11]. An orbital contribution of  $\chi_{orb} = 6 \times 10^{-5} \text{ emu/mol}$  has been subtracted from all data shown ( $M_m = M - \chi_{orb}H$ ).

Figure 1 shows the temperature-concentration phase diagram. For  $x \leq 11\%$ , the critical temperature  $T_c$  was determined by the standard Arrott analysis. Plots of  $M^2$  vs.  $H/M$  as in Fig. 2 show straight parallel isotherms which implies  $M^2 = M_0^2(T) + cH/M$  as is common for itinerant magnets (in Fig. 2, only low  $T$  data are shown).  $T_c$  is then extracted via the mean-field  $T$ -dependencies of  $M_0(T)$  and susceptibility ( $-c/M_0^2(T)$ ) [12]. The resulting  $T_c(x)$  can be simply extrapolated linearly (dashed line) from the high  $T_c = 630\text{K}$  of nickel down to 0 at  $x \approx 11\%$  [8].

For  $x \geq 11\%$ , the straightforward AP analysis does not longer work because the data in Fig. 2 are not described by straight lines. Introducing “exponents” as in a classical critical regime leads to a “modified” Arrott plot [13] implying the behavior  $M^{1/\beta} = M_0^{1/\beta}(T) + c(H/M)^{1/\gamma}$ . A good description for  $x > 11\%$  of the  $M(H > 0.5T, T)$  data in a wide regime (outside any critical regime) can be achieved with  $\beta = 0.5$  and  $\gamma(x) < 1$  [12], as indicated by the dotted fit line in

Fig. 2. The resulting transition temperatures  $T_c^*$  of these modified Arrott plots remain finite up to  $x = 15\%$ , while other extrapolations in Fig. 2 using smaller  $H/M$  values would lead to smaller  $T_c$ .

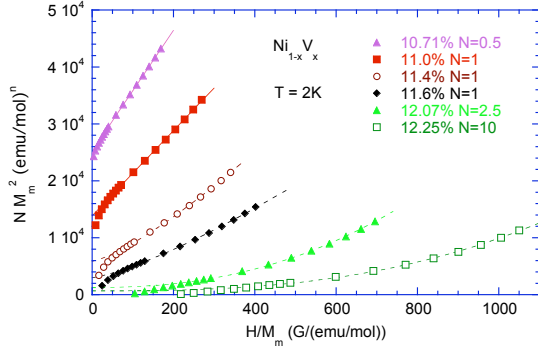


**Figure 2.** Probing Arrott plots ( $M^2 - M_0^2 \sim (H/M)^{1/\gamma}$  with  $\gamma = 1$ ) for various V-concentrations  $x$ . For clarity only low temperature  $T = 2K$  data (with modified y-value) are shown. For  $x > 11\%$  a modified Arrott plot (with  $\gamma(x) < 1$ ) is a good description of the data above  $H \approx 0.5T$  as indicated by the dashed line.

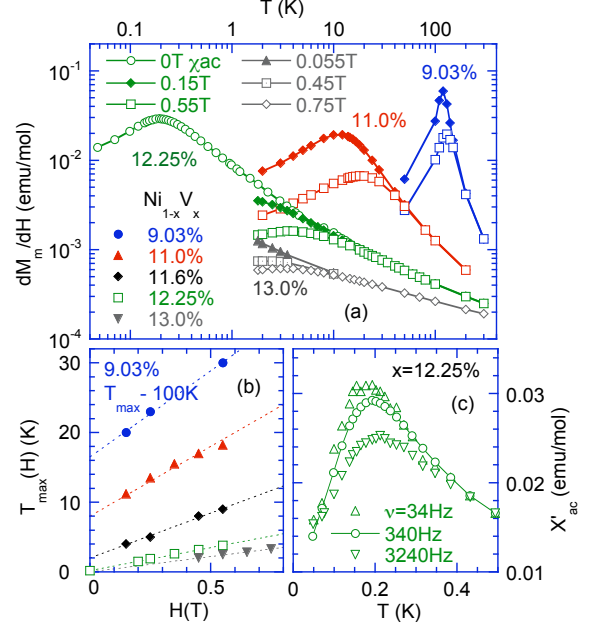


**Figure 3.** Determination of transition temperature  $T_{max}$ . (a) Differential susceptibility  $dM_m/dH$  vs temperature  $T$  in small magnetic fields  $H$  (symbol) displaying maxima at  $T_{max}(H)$  for different  $x$ . (b)  $T_{max}(H)$  vs magnetic field  $H$ . The dashed line indicates the linear extrapolation to determine  $T_{max} = T_{max}(H \rightarrow 0)$ . (c) ac-susceptibility  $\chi'_{ac}$  vs. temperature  $T$  in  $H = 0T$  with  $H_{ac} = 0.1G$  at different frequencies  $\nu$  for  $x = 12.25\%$ .

In addition to Arrott plots, we analyze field-dependent maxima at  $T_{max}(H)$  in the differential susceptibility  $\chi(T) = dM(T)/dH$  indicating spin ordering or freezing as shown in Fig. 3(a). Fig. 3(b) shows the linear extrapolation of  $T_{max}(H)$  taken at  $0.55T$  to  $0.1T$  to determine  $T_{max} = T_{max}(H \rightarrow 0)$ . In particular for  $x = 12.25\%$  a frequency dependent maximum at  $T_{max} = 0.19K$  was determined by  $\chi_{ac}(T, \nu = 380Hz)$  in zero field with  $H_{ac} = 0.1G$  which hints at the onset of a cluster glass [11].  $T_{max}$  increases by  $0.018K$  per decade in frequency [11] as shown in Fig.3(c). Although a detailed study of the evolution with dilution  $x$  of the cluster growth and dynamics is still outstanding, we can already note the qualitative effects of disorder on the ferromagnetic ordered state for  $x > 11\%$ . As is obvious in Fig. 1, the high and low field extrapolation lead to *different* transition temperatures ( $T_c, T_c^* > T_{max}$ ) hinting at cluster freezing for  $x > 11\%$ . The  $x$ -dependence of  $T_{max}$  in the accessible temperature region is better described by an exponential (dotted line) rather than a power law. Also, a “tail” fit to  $(\ln(T/T_0) \sim (x_c - x)^{-\nu\psi})$ , see [14]) rather than a power law serves as a good description of the onset of FM order for data between about 9% and 11% leading to  $x_c \approx 11.6\%$  (solid line). The discrepancies between the various methods and the spin-glass like features at the lowest temperatures suggest that the real QCP is masked at very low  $T$  by ordering of clusters.

Nonetheless, at sufficiently high temperatures (in the region  $T_{max} < T < T_c(0\%)$ ) cluster ordering does not seem to play a role, and various quantities display power laws. Figs. 4(a) and (b) present the  $H$  and  $T$  dependencies of the magnetization as  $M/H$  for various  $x$ . Fig. 4(b) shows essentially the susceptibility  $\chi$ , since  $\chi = M/H = dM/dH$  for low fields ( $H < 0.5T$ ) and high  $T$  ( $T > 20K$ ,  $T > T_c$ ). While for  $x \leq 11\%$  the negative slope in the log-log plot  $\gamma = -d\ln(\chi_m)/d\ln(T)$  increases with falling  $T$  towards  $T_c$ , for  $x > 11\%$ ,  $\chi(T)$  follows a simple power law for  $20K < T < 300K$ . The exponent decreases from  $\gamma(x = 11.4\%) = 1$  to  $\gamma(x = 15\%) = 0.04$ .  $M/H(H)$  follows a power law  $M/H \sim H^{\alpha-1}$  for high  $H$ . For  $x < 11\%$ , where  $M(H)$  nearly saturates, the exponent  $1 - \alpha$  is close to 1, and therefore very different than  $\gamma$ . However, for  $x > 12\%$ , the high-field exponent  $1 - \alpha$  matches the susceptibility exponent  $\gamma$ . The deviations from a power law at low fields in Fig. 4(a) are due to the finite  $T$  limitations.

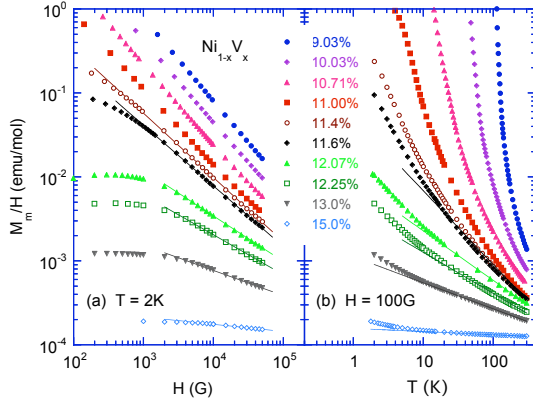


**Figure 4.** (a) Magnetic field  $H$  and (b) temperature  $T$  dependence of the magnetization  $M$  for a wide  $x$  regime.  $M/H(H, T)$  follows a power law (solid line) with the same exponent  $(\alpha - 1)$  in (a) as  $(\gamma)$  in (b) for all  $x > 11.6\%$ .

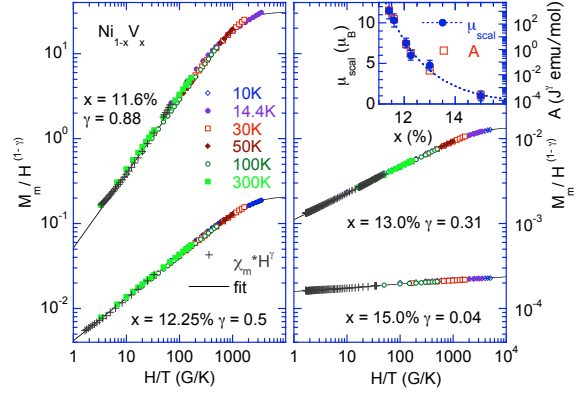


**Figure 5.**  $H/T$  scaling plot showing some  $M(H, T)$  data within  $10K - 300K$  and  $100G - 50kG$  for different  $x$ . The line represents a fit using  $Y(z)$  (see text). Inset shows fit parameters  $\mu_{scal}$  and  $A$  vs  $x$ .

Since both the  $M(T)$  and  $M(H)$  show power laws with the same exponent, simple  $H/T$  scaling is expected for  $x > 12\%$ . Fig. 5 shows the scaling plot using the form  $M/H = H^{-\gamma} Y(\mu_{scal} H/k_B T)$  where  $Y$  is the scaling function and  $\mu_{scal}$  is a scaling moment for several  $x$ . All  $M(H, T)$  data for  $T \geq 14K$  collapse, confirming  $H/T$  scaling. The scaling function  $Y$  is well approximated by the form  $Y(z) = A'/(1 + z^{-2})^{\gamma/2}$  where  $A' = A/\mu^\gamma$  is a constant. This phenomenological form arises from simply combining the two limiting power laws with the same exponent  $\gamma$  in the  $H - T$  plane,  $(M/H)^{-1} = H^\gamma Y^{-1} \sim [(\mu_{scal} H)^2 + (k_B T)^2]^{\gamma/2}$ . Close to  $x = 11.6\%$ , the quality of the collapse is less satisfactory. The resulting exponent  $\gamma$  (which matches that obtained by a fit of  $\chi(T)$  for all  $x$  between  $11.4\%$  and  $15\%$ ) is shown in the inset of Fig. 1. The scaling moment  $\mu_{scal}$  and amplitude  $A$  are shown in the inset of Fig. 5, demonstrating the growth of the typical cluster size and number with  $x \rightarrow x_c$ .

The consistent power laws, and in particular, the  $H/T$  scaling of  $M(H, T)$  are in excellent agreement with the predictions for a quantum Griffiths phase with Griffiths exponent  $\lambda = \alpha = 1 - \gamma$ . A critical concentration of  $x_c = 11.4\%$  can be identified from the condition  $\gamma(x_c) = 1$  (neglecting logarithmic terms). Fitting to power law  $1 - \gamma(x) \sim (x - x_c)^{\nu\psi}$  as predicted by theory [3] yields  $x_c = 11.6\%$  with  $\nu\psi = 0.42$  as shown in the upper inset in Fig. 1. This value is in close agreement with the “tail” fit of  $T_{max}(x)$ .

### 3. Conclusions

On the one hand, our results confirm that  $\text{Ni}_{1-x}\text{V}_x$  follows the scenario of an infinite-randomness QCP with a quantum Griffiths phase, as expected in an itinerant Heisenberg magnet [3, 4]. The QCP at  $x_c \approx 11.6\%$  has been estimated by extrapolations from outside the critical region, where the cluster ordering is less disturbing (through  $\gamma(x_c) \rightarrow 1$  and  $T_{max}(x_c) \rightarrow 0$ ). On the other hand, we see clear signs of cluster ordering towards  $x_c$ , in particular deviations from scaling at lower temperatures (such as the upturns in Fig. 4(a) as well as model dependent transition temperatures for  $x > 11\%$ ). As discussed in Ref. [11], the magnetization  $M(H, T > T_{max})$  for  $x > 12\%$  can be well described by an additional “Curie term” due to frozen clusters which exceeds the term due to the fluctuating (Griffiths) clusters below  $T_{cross}$  (see Fig. 1). Such a change in low-temperature behavior was predicted to occur in itinerant Heisenberg systems due to the RKKY interactions [15]. A Griffiths phase with nonuniversal power laws at higher  $T$  (but below  $T_c(0\%)$ ) combined with a cluster glass (CG) (indicated by maxima in  $\chi(T)$ ) at very low  $T$  has also been observed in other diluted compounds ( $\text{CePd}_{1-x}\text{Rh}_x$  [7],  $\text{URu}_{2-x}\text{Re}_x\text{Si}_2$  [16]) close to a ferromagnetic transition with much lower  $T_c$  and can be understood as a generic feature of this disordered itinerant QPT [14].

This work has been supported in part by the NSF under grant nos. DMR-0306766, DMR-0339147, and DMR-0906566 and by Research Corporation.

### References

- [1] v Löhneysen H, Rosch A, Vojta M and Wölfle P 2007 *Reviews of Modern Physics* **79** 1015
- [2] Vojta T 2006 *J. Phys. A.: Math. Gen.* **39** R143
- [3] Hoyos J A, Kotabage C and Vojta T 2007 *Phys. Rev. Lett.* **99** 230601; Vojta T, Kotabage C and Hoyos J A 2009 *Phys. Rev. B* **79** 024401
- [4] Vojta T and Schmalian J 2005 *Phys. Rev. B* **72** 045438
- [5] Stewart G R 2001 *Rev. Mod. Phys.* **73** 797; Stewart G R 2006 *Rev. Mod. Phys.* **78** 743
- [6] Castro Neto A H and Jones B A 2000 *Phys. Rev. B* **62** 14975
- [7] Westerkamp T, Deppe M, Kuchler R, Brando M, Geibel C, Gegenwart P, Pikul A P and Steglich F 2009 *Phys. Rev. Lett.* **102** 206404
- [8] Bölling F 1968 *Phys. Kondens. Mater.* **7** 162
- [9] Friedel J 1958 *Nuovo Cimento* **7** 287
- [10] Nicklas M, Brando M, Knebel G, Mayr F, Trinkl F and Loidl A 1999 *Phys. Rev. Lett.* **82** 4268
- [11] Ubaid-Kassis S, Vojta T and Schroeder A 2010 *Phys. Rev. Lett.* **104** 066402
- [12] Ubaid-Kassis S and Schroeder A 2008 *Physica B* **403** 1325
- [13] Arrott A and Noakes J E 1967 *Phys. Rev. Lett.* **19** 786
- [14] Vojta T 2010 *J. Low Temp. Phys.* **161** 299
- [15] Dobrosavljević V and Miranda E 2005 *Phys. Rev. Lett.* **94** 187203
- [16] Bauer E D, Zapf V S, Ho P C, Butch N P, Freeman E J, Sirvent C and Maple M B 2005 *Phys. Rev. Lett.* **94** 046401